DYNAMIC, LARGE-DEFLECTION, INELASTIC AND THERMAL STRESS ANALYSIS BY THE FINITE ELEMENT METHOD

W.E. HAISLER, J.A. STRICKLIN

Aerospace Engineering Department,
Texas A & M University, College Station, Texas 77843, U.S.A.

SUMMARY

A finite element theory and computer program have been developed for predicting the dynamic, large displacement, inelastic and thermal response of stiffened and layered structures. The dependence of material properties on temperature is explicitly accounted for and any arbitrary, transient mechanical or thermal load history is allowed. The shell may have internal or external stiffeners and be constructed with up to three layers. The equations of motion are developed by using the pseudo force approach to represent all nonlinearities and are then solved by using either the Houbolt method or central differences. Moderately large rotations are allowed.

The program is based on an incremental theory of plasticity using the Von Mises yield condition and associated flow rule. The post yield or work-hardening behavior is idealized with either the isotropic hardening or mechanical sublayer models. Two models are utilized since it has been found through comparison with experimental results that isotropic hardening is best for simple loading conditions while the mechanical sublayer model is better for reverse and cyclic loading. Strain-rate effects are also accounted for in the program by using a power-law type model based on the strain rate. The dependence of material properties on temperature is taken into account in the pseudo forces. Young's modulus, Poisson's ratio, thermal coefficient of expansion, the yield stress, and the entire stress strain curve are treated as functions of the applied temperature.

The theory and program have been used to successfully solve a number of significant problems. Containment vessels subjected to transient and shock-type mechanical and thermal loads have been analyzed. Both symmetric and unsymmetric loadings have been treated. Using the program, good agreement has been observed with experimental and other analytical methods (where available). Results have been obtained for a number of thermal loading and materially thermal dependent problems. In particular, results are presented for one case with a temperature load varying from 600 to 2000°F. Because of the high temperatures, extensive plastic flow in the inelastic region is experienced.

In summary, the significant results presented in this paper are: (1) the development of a finite element theory to treat nonlinear, inelastic, thermal response of structures with temperature dependent material properties and (2) the demonstration of the theory and program through the solution of several complex, highly nonlinear structures subjected to severe mechanical and thermal transient loadings.

1. Introduction

Significant advancements have been made in the last ten years in the development and application of theory to the large deflection, inelastic response of complex structures. This has been brought about for primarily two reasons: a better understanding of the physical principles envolved and the ever-increasing advances in computer technology providing faster execution times, greater accuracy, and larger storage capacity. Of course, this rapid development has been somewhat pushed along by the need to understand what happens to structures when subjected to intense impact loads, high temperatures, accident conditions, and the like. This is particularly true of the nuclear industry where nuclear components must be designed to survive accidents even though the probability of such accidents is extremely low.

A number of computer codes have already been developed for large-deflection, inelastic structural response. Many of these are tabulated in the proceedings of the International Symposium on Structural Mechanics Software [1]. For thin shell structures, the most widely used finite difference codes have been developed by the research groups at M.I.T. [2,3], Ballistic Research Laboratories [4-6], Sandia Laboratories [7,8] and Lockheed [9,10]. Finite element shell programs have been developed by McNamara and Marcal [11], Wu and Witmer [12], and Stricklin, et al. [13]. General purpose codes are also available [1]; however, the nonlinear capability of many of these general purpose codes is somewhat limited.

The present paper represents an extension of earlier work reported in references [14,15] in which the DYNAPLAS II computer program is developed for the transient, nonlinear response of ring stiffened shells of revolution. A paper to be presented by VonRiesemann [16] at this conference outlines the capabilities and limitations of this program and presents solutions to several engineering problems obtained with DYNAPLAS II. The purpose of this paper is to present the finite element theory and associated computer program, DYNAPLAS III, which have been developed for predicting the dynamic, large displacement, inelastic and thermal response of stiffened and layered thin shell structures. The dependence of material properties on temperature is explicitly accounted for and any arbitrary transient mechanical or thermal loading history is allowed. Solutions to several problems are presented to demonstrate the capability of the computer program.

2. Formulation

There are several different approaches that may be used to formulate the materially and geometrically nonlinear problem. These include the total Lagrangian formulation based on the 2nd Piola-Kirchhoff stress and Green-Lagrangian strain tensors, the updated Lagrangian formulation, and Eulerian or moving coordinate formulations. Stricklin [25] has previously discussed the differences in these various approaches. It should be noted that the 2nd Piola-Kirchhoff stress tensor, although referred to as the stress, is not a true stress accept for small strains. In general the Cauchy stress is preferred for large strain problems.

The formulation used herein is based on the total Lagrangian coordinate system. The basic starting point for this formulation is the equations of equilibrium written in terms of the 2nd Piola-Kirchhoff stress [17]

$$\frac{\partial}{\partial a_j}\left[S_{jk}\left(\delta_{ik}+\frac{\partial u_i}{\partial a_k}\right)\right]+\rho_o F_{oi}=\rho_o \ddot{u}_i \tag{1}$$

where

S_{jk} = 2nd Piola-Kirchhoff stress tensor
a_i = coordinate in original body
u_i = Lagrangian displacement
$\rho_o F_{oi}$ = body force
δ_{ik} = Kronecker delta
$\ddot{u}_i$ = acceleration

Multiplying eq. (1) by a virtual displacement δu_i (index summation noted) and integrating over the undeformed body yields equations of equilibrium in the form

$$\int_{V_o}\rho_o \ddot{u}_i \delta u_i dV+\int_{V_o}[S]\{\delta\varepsilon\}dV=\delta W^* \tag{2}$$

where

$[S]$ = 1 x 6 matrix of 2nd Piola-Kirchhoff stresses
$\{\varepsilon\}$ = 6 x 1 matrix of Green or Lagrangian strains

$$\varepsilon_{ij}=\frac{\partial u_i}{\partial a_j}+\frac{\partial u_j}{\partial a_i}+\frac{\partial u_k}{\partial a_i}\frac{\partial u_k}{\partial a_j} \qquad i\neq j$$

$$\varepsilon_{ij}=\frac{\partial u_i}{\partial a_j}+\frac{1}{2}\frac{\partial u_k}{\partial a_i}\frac{\partial u_k}{\partial a_j} \qquad i=j \tag{3}$$

δW^* = virtual work done in deformed body
V_o = volume of undeformed body.

The derivation of eq. (2) from eq. (1) follows exactly the same procedure as for the small deflection case presented by Argyris [18]. Obtaining the virtual work in the deformed body, δW^*, requires a physical interpretation of the Kirchhoff stress tensor as presented in Malvern [19] and, in more detail, by Haisler [20].

Restricting attention to small strains, the Kirchhoff stress is the true stress and is related to the elastic component of the Green strains through the matrix $[D]$

$$\{S\}=[D]\{\varepsilon^e\} \tag{4}$$

where the $[D]$ matrix is dependent on the temperature and is based on material properties at the current temperature.

As small strains are assumed, the total strain is the linear superposition of the various components.

$$\{\varepsilon\}=\{\varepsilon^e\}+\{\varepsilon^P\}+\{\varepsilon^T\}+\ldots \tag{5}$$

where the three terms on the right side of eq. (5) are the elastic, plastic, and thermal components, respectively, of the total strain. Solving eq. (5) for the elastic strain, substituting into eq. (4), and substituting the result into eq. (2) yields:

$$\int_{V_o}\rho_o \ddot{u}_i \delta u_i dV+\int_{V_o}\left([\varepsilon]-[\varepsilon^P]-[\varepsilon^T]-\ldots\right)[D]\{\delta\varepsilon\}=\delta W^* \tag{6}$$

For some problems, the potential due to external forces may be a higher order function of the displacements; but, as usual, the assumption of a first-order function of the

displacements is assumed herein and consequently

$$W^* = \lfloor q \rfloor \{P(t)\} \tag{7}$$

where $\{P\}$ are externally applied forces. Hence

$$\delta W^* = \lfloor P \rfloor \{\delta q\} \tag{8}$$

Taking the variation of eq. (6) with respect to generalized coordinate q_i yields the equations of equilibrium:

$$\int_{V_o} \rho_o \ddot{u}_j \frac{\partial u_j}{\partial q_i} dV + \int_{V_o} \left\lfloor \frac{\partial \epsilon}{\partial q_i} \right\rfloor [D]\{\epsilon\} dV - \int_{V_o} \left\lfloor \frac{\partial \epsilon}{\partial q_i} \right\rfloor [D]\{\epsilon^P\} dV$$

$$\int_{V_o} \left\lfloor \frac{\partial \epsilon}{\partial q_i} \right\rfloor [D]\{\epsilon^T\} dV - \ldots = \{P\} \tag{9}$$

It is convenient to write the total strain as

$$\epsilon = \epsilon_L + \epsilon_{NL} \tag{10}$$

where ϵ_L and ϵ_{NL} are the linear and nonlinear contributions, respectively, to the total strain. Substituting eq. (10) into eq. (9) and expanding the second term on the left-hand side, yields

$$\int_{V_o} \rho_o \ddot{u}_j \frac{\partial u_j}{\partial q_i} dV + \int_{V_o} \left\lfloor \frac{\partial \epsilon_L}{\partial q_i} \right\rfloor [D]\{\epsilon_L\} dV + \int_{V_o} \left\lfloor \frac{\partial \epsilon}{\partial q_i} \right\rfloor [D]\{\epsilon_{NL}\} dV$$

$$+ \int_{V_o} \left\lfloor \frac{\partial \epsilon_{NL}}{\partial q_i} \right\rfloor [D]\{\epsilon_L\} dV - \int_{V_o} \left\lfloor \frac{\partial \epsilon}{\partial q_i} \right\rfloor [D]\{\epsilon^P\} dV - \int_{V_o} \left\lfloor \frac{\partial \epsilon}{\partial q_i} \right\rfloor [D]\{\epsilon^T\} dV - \ldots = P_i \tag{11}$$

In eq. (11), the $[D]$ matrix is assumed to be a known function of temperature. It is convenient to let $[D_o]$ be the value of $[D]$ at some unstressed, reference (room) temperature and to rewrite the second term of eq. (11) in terms of $[D_o]$ and $[D]$ so that

$$\int_{V_o} \rho_o \ddot{u}_j \frac{\partial u_j}{\partial q_i} dV + \int_{V_o} \left\lfloor \frac{\partial \epsilon_L}{\partial q_i} \right\rfloor [D_o]\{\epsilon_L\} dV$$

$$- \int_{V_o} \left\lfloor \frac{\partial \epsilon_L}{\partial q_i} \right\rfloor [D_o]\{\epsilon_L\} dV + \int_{V_o} \left\lfloor \frac{\partial \epsilon_L}{\partial q_i} \right\rfloor [D]\{\epsilon_L\} dV + \int_{V_o} \left\lfloor \frac{\partial \epsilon}{\partial q_i} \right\rfloor [D]\{\epsilon_{NL}\} dV$$

$$+ \int_{V_o} \left\lfloor \frac{\partial \epsilon_{NL}}{\partial q_i} \right\rfloor [D]\{\epsilon_L\} dV - \int_{V_o} \left\lfloor \frac{\partial \epsilon}{\partial q_i} \right\rfloor [D]\{\epsilon^P\} dV - \int_{V_o} \left\lfloor \frac{\partial \epsilon}{\partial q_i} \right\rfloor [D]\{\epsilon^T\} dV - \ldots = P_i \tag{12}$$

The first term in eq. (12) produces the terms of the mass matrix times the accelerations. The second term gives the contribution to the usual linear stiffness matrix times the generalized coordinate (both based on material properties at the reference temperature). The remaining terms may be combined to yield

$$m_{ij}\ddot{q}_j + k_{ij}q_j = P_i - \int_{V_o} \left\lfloor \frac{\partial \epsilon_L}{\partial q_i} \right\rfloor [D]\{\epsilon_L\} dV + \int_{V_o} \left\lfloor \frac{\partial \epsilon_L}{\partial q_i} \right\rfloor [D_o]\{\epsilon_L\} dV$$

$$- \int_{V_o} \left\lfloor \frac{\partial \epsilon_{NL}}{\partial q_i} \right\rfloor [D]\{\epsilon_L\} - \int_{V_o} \left\lfloor \frac{\partial \epsilon}{\partial q_i} \right\rfloor [D]\{\epsilon_{NL} - \epsilon^P - \epsilon^T - \ldots\} dV \tag{13}$$

where

$$m_{ij} = \int_{V_o} \rho_o \frac{\partial u_k}{\partial q_i} \frac{\partial u_k}{\partial q_j} dV \tag{14}$$

$$k_{ij} = \int_{V_o} \left[\frac{\partial \varepsilon_L}{\partial q_i}\right] [D_o] \left\{\frac{\partial \varepsilon_L}{\partial q_j}\right\} dV \tag{15}$$

It should be noted that the volume integrals extend over the entire region affected by q_i and q_j. This integration is, of course, performed by integrating over each element separately (including all layers and ring stiffness) and assembling the results in the standard manner for all elements.

Writing eq. (13) for each and every degree of freedom yields the complete set of equilibrium equations in matrix form

$$[M]\{\ddot{q}\} + [K]\{q\} = \{P\} + \{Q^*\} \tag{16}$$

where

$$Q_i^* = -\int_{V_o} \left[\frac{\partial \varepsilon_L}{\partial q_i}\right] [D]\{\varepsilon_L\} dV + \int_{V_o} \left[\frac{\partial \varepsilon_L}{\partial q_i}\right] [D_o]\{\varepsilon_L\} dV$$
$$- \int_{V_o} \left[\frac{\partial \varepsilon_{NL}}{\partial q_i}\right] [D]\{\varepsilon_L\} dV - \int_{V_o} \left[\frac{\partial \varepsilon}{\partial q_i}\right] [D]\{\varepsilon_{NL} - \varepsilon^P - \varepsilon^T \ldots\} dV \tag{17}$$

The last term on the right side of eq. (16) is generally called the pseudo force and is a function of the unknown displacements.

In eq. (17) the pseudo forces due to material and geometric nonlinearities are included together instead of separating them into components. The separate components are given as:

$$Q_i^* = Q_i^I + Q_i^{NL} \tag{18}$$

where

Q^I = pseudo force due to initial (plastic and thermal) strains
Q^{NL} = pseudo force due to geometric nonlinearities

$$Q_i^I = \int_{V_o} \left[\frac{\partial \varepsilon}{\partial q_i}\right] [D]\{\varepsilon^P + \varepsilon^T + \ldots\} dV - \int_{V_o} \left[\frac{\partial \varepsilon_L}{\partial q_i}\right] [D]\{\varepsilon_L\} dV + \int_{V_o} \left[\frac{\partial \varepsilon_L}{\partial q_i}\right] [D_o]\{\varepsilon_L\} dV \tag{19}$$

$$Q_i^{NL} = -\int_{V_o} \left[\frac{\partial \varepsilon_{NL}}{\partial q_i}\right] [D]\{\varepsilon_L\} dV - \int_{V_o} \left[\frac{\partial \varepsilon}{\partial q_i}\right] [D]\{\varepsilon_{NL}\} dV$$
$$= -\int_{V_o} \left[\frac{\partial \varepsilon_L}{\partial q_i}\right] [D]\{\varepsilon_{NL}\} dV - \int_{V_o} \left[\frac{\partial \varepsilon_{NL}}{\partial q_i}\right] [D]\{\varepsilon\} dV \tag{20}$$

In eqs. (19) and (20) the [D] matrix is based on the current temperature and may vary from layer to layer in the shell. The volume, V, is taken to be that of all the shell layers plus any ring stiffeners on the element. The last form of eq. (20) is the more efficient from the computational point of view when only geometric nonlinearities are considered. Furthermore, within the realm of shell analysis, eq. (20) may be integrated through the thickness of the shell. The approximate expressions, assuming moderate rotations, for the total strain in the shell with the ring stiffener being a special case is given by:

$$\{\varepsilon\} = \{e\} + \{\varepsilon_{NL}\} + n\{\kappa\} \tag{21}$$

where $\{e\}$ are the usual expressions for the linear membrane strains, $\{\kappa\}$ are the changes in curvature and twist and n is the distance from the reference surface.

Substituting eq. (21) into the second form of eq. (20) and integrating through the thickness yields

$$Q_i^{NL} = -t\int_{A_o}\left[\frac{\partial e}{\partial q_i} + \bar{n}\frac{\partial \kappa}{\partial q_i}\right][D]\{\varepsilon_{NL}\}dA - t\int_{A_o}\left[\frac{\partial \varepsilon_{NL}}{\partial q_i}\right][D]\{e + \varepsilon_{NL} + \bar{n}\kappa\}dA \tag{22}$$

where t is the thickness and $\bar{n}$ is the distance from the reference surface to the centroid of the layer under consideration. In the present research, the reference surface is assumed to be any convenient surface, i.e., midsurface symmetry of the shell layers is not required. Likewise, the circumferential ring stiffeners may be eccentrically located on the shell surface.

The basic governing equations are (16), (19), and (22). It should be observed that the pseudo forces in eq. (16) are functions of the displacements and hence vary with time. The computational aspects of solving these equations is discussed in the next section.

3. Computational Considerations

The general shell formulation presented in the previous section has been specialized to thin shells of revolution. These details are given in reference [14] and will be only summarized here. The linear stiffness matrix [K] and mass matrix [M] in eq. (16) are obtained based on orthotropic material and neglecting transverse shear deformations. The displacement functions are assumed to be cubic polynomials in the meridional direction and Fourier series in the circumferential direction resulting in an eight degree-of-freedom element per Fourier harmonic. The computer program permits each element to be constructed of up to three layers each of which may have different material properties. The ring stiffeners may be eccentrically located and may be made up of three flanges.

The nonlinear pseudo force terms are evaluated approximately using finite difference approximations for the strains and numerical integration over the volume of each element [14]. It should be pointed out that, although a Fourier series type solution is being used, all coupling between the Fourier harmonics is contained in the pseudo force term on the right side of eq. (16), i.e., the left hand side of the equation is uncoupled.

The computer program is based on the incremental theory of plasticity using the Von Mises yield condition and associated flow rule. The post yield or work-hardening behavior of the material is taken into account through the isotropic model [21] or the mechanical sublayer model [22]. A recent numerical-experimental correlation study [23] has shown that for most loading paths, isotropic hardening yields the best results. However, for reversed loadings the mechanical sublayer model was found to better fit most observed experimental data.

The material parameters including Young's modulus, Poisson's ratio, yield stress, coefficient of thermal expension and the entire uniaxial stress-strain curve are assumed to be functions of temperature. These are input as a function of temperature in tabular form into the computer program. As the numerical integration of the pseudo forces is performed, the value of of each material parameter is determined for the temperature at

that integration station.

The applied loading may be any arbitrary, transient mechanical or thermal load history.

The equations of motion are integrated numerically using Houbolts method although the computer program allows the user to optionally select the central difference method. The Houbolt method is reasonably accurate and the artificial damping permits the pseudo force terms in eq. (16) to be extrapolated from the previous time step without appreciable loss of accuracy.

The computer program is written in the FORTRAN IV language and has been executed on the IBM 360/65, Unival 1108 and CDC 6600 and 7600 computers. Copies of the user's manuals and computer program are available upon request. Requests should be addressed to Dr. Walter E. Haisler, Aerospace Engineering Department, Texas A&M University, College Station, Texas 77843, U.S.A.; Phone (713) 845-7541.

4. Numerical Solutions

The purpose of this section is to present the numerical solutions obtained for several problems using the DYNAPLAS III computer program. The solutions show the versatility of DYNAPLAS III as well as its limitations.

4.1 Truncated Cone Under Half-Cosine Impulse.

The first problem considered is the large deflection elastic-plastic dynamic response of a truncated cone under a half cosine impulsively applied pressure. The truncated cone has an upper radius of 7.95 in., a lower radius of 10.23 in., a thickness of 0.5430 in., and a density of 1.88×10^{-4} lb-sec^2/in.^{4} Additional details are given on Fig. 1. The material was assumed to have a yield stress of 30,000 psi and to be elastic-perfectly plastic.

In Fig. 1, results are presented for the deflections obtained for DYNAPLAS, REPSIL[5], and SHORE [9]. Considering the fact that the three computer codes are completely independent, the agreement of displacements is considered to be outstanding and serves as a check on the accuracy of all three codes. Similar agreement was obtained for the strains. However, based on the shown displacements, it is clear that the degree of geometric nonlinearity is not severe.

In DYNAPLAS, the conical frustum shell was idealized as 30 equally spaced finite elements and 10 Fourier terms were used. Seven Simpson stations were used through the thickness and a 2-μsec time step was used. Two runs were made varying the frequency of updating the pseudo forces and the number of modified Simpson stations around the circumference. Results were the same for both cases. In the first, 13 Simpson stations were used and the pseudo forces were updated every three time increments with an extrapolation factor of 1.0. The computer run time was 10 min. on the CDC 6600. In the second run, 17 Simpson stations were used and the pseudo forces were updated every time increment. The computer run time was 30 min. on the CDC 6600. Storage requirements were 88,000 words for the second case.

The SHORE code was run using 30 and 18 equally spaced increments along the meridian and around the circumference, respectively. The computer run time was 22½ min. on the UNIVAC 1108 which is comparable to the first run for DYNAPLAS.

4.2 Circular Plate with Impulsive Load

The second example is the analysis of an impulsively loaded circular plate tested

experimentally by Duffey and Key [24]. The plate was idealized with eleven elements. The uniaxial stress-strain curve was represented by a 3 segment piece-wise linear curve: an initial elastic modulus of 10.4×10^6 psi to a total strain of 0.00424 in/in, then a secondary modulus of 3.29×10^6 psi to a total strain of 0.00449 in/in, and perfectly plastic behavior thereafter. The problem was solved using both the isotropic and mechanical sublayer work-hardening models.

The experimental and theoretical results for the center axial deflection are shown in Fig. 2. Good agreement is achieved up to the initial peak deflection and over part of the unloading curve. However, the experimental results deviate from the theoretical results beyond about 450 μ seconds; probably due to the significant unloading present.

For demonstration purposes, the plate was also considered as made of two equal layers; the top half of steel and the bottom half of aluminum. The uield stress of the steel layer was taken as 127,000 psi with an ulitmate stress of 135,000 psi. As expected the deflections are somewhat smaller since the plate is stiffer.

4.3 Thermal Shield

The next problem is the solution of a heat shield (Fig. 3) subjected to "slowly" applied, symmetric thermal load which varies from 600°F at the crown to 2000°F at the tip. As seen in Fig. 3, the structure is essentially a flat plate with a varying thickness. The structure was idealized using 21 elements. The supporting ring at r=2.5" was ignored and replaced by a simple support boundary condition not allowing vertical motion.

The temperature was assumed to be uniform through the thickness and to vary linearly from 600°F at the crown to 2000°F at the tip. The thermal load was applied "slowly" from zero to the final values over a period of 2.5 milliseconds.

The plate was assumed to be constructed of high strength stainless steel with room temperature properties: $E=30 \times 10^6$ psi, $G=11.5 \times 10^6$ psi, $\nu=0.3$, $\rho=0.3$ lb/in^3, yield strength of 145,000 psi, and ultimate strength of 180,000 psi. The strain-hardening stress-strain curve was approximated using 4 piece-wise linear curve with perfectly plastic behavior at the ultimate stress. At 2000°F, the Young's modulus, yield stress and ultimate stress have decreased to about 12.5×10^6 psi, 10,000 psi and 16,000 psi, respectively.

The solution was obtained using Houbolts method with a time step of 25 μ seconds and using the isotropic hardening model. Geometric nonlinearities were neglected. Rather than letting the material properties vary with temperature in this case, the values corresponding to the final temperature for each element were used and held constant throughout the loading.

Figure 3 shows the meridional and circumferential stress at the lower surface of the heat shield at a time of 5.5 milliseconds (corresponds to time of peak stress). Although the temperature at the tip is quite high (2000°F), the stress is low since the modulus and yield stress of the material have been reduced appreciably at that point. Because of the high temperatures, the outermost 3 inches at the tip goes entirely plastic while the enterior region ($r \leq 7$") remains elastic.

4.4 Cylindrical Baffle with Applied Temperature

The last problem considers the cylindrical shell shown in Fig. 4 subjected to a combined static internal pressure and suddenly applied concentrated heating. The shell is assumed to be constructed of an alunimum-type material with room temperature properties:

$E=10 \times 10^6$ psi, $\nu=0.3$, $\rho=0.1$ lb/in^3, and perfectly plastic with a yield strength of 40,000 psi. At a temperature of 600°F, Young's modulus and the yield stress are assumed to decrease to 70% and 30%, respectively, of their room temperature values.

The shell was idealized using 20 elements and 5 Fourier terms. To first obtain the static solution to a 400 psi internal pressure, the load was applied slowly over a period of 20 milliseconds. Using a time step of 1 millisecond, Houbolt's method damps the dynamic solution to the static values as shown in Fig. 4. The load was then held constant until 30 milliseconds and then a spot thermal load was applied at a point 20 inches from the top of the cylinder. The temperature on the outside surface was increased from 0°F to 500°F as a ramp function reaching its peak value after 50 microseconds (constant thereafter). The inside surface temperature was assumed to remain unchanged so that a temperature gradient developed through the thickness. In the circumferential direction, the spot was approximated as being a half-cosine. In the meridional direction, the load was applied over a 10 inch length centered at Z=20 inches and varying as a sine function as shown in Fig. 4. The response to the thermal loading was obtained by restarting the program at 30 milliseconds and using a time step of 1 microsecond.

Figure 4 shows th circumferential stress response under the spot heating. The stress is initially at its static value of 28,000 psi and then drops rapidly to about -29,000 psi as the shell is heated. Although the stress responds almost instantaneously to the heating, the structural response is much slower. As seen in Fig. 5, the radial deflection does not reach its peak until some 600 microseconds after the temperature has reached its peak. Figure 6 shows the radial deflection around the circumference at a time of 30.61 milliseconds when the peak displacement has been reached. The displacements increase significantly under the spot heating but are relatively unaffected on the opposite side of the shell where the displacements are about equal to that due to the internal pressure.

Acknowledgement

This research was supported under Sandia Laboratories Contract 82-7739 and ONR Contract N00014-68-A-0308-004. Appreciation is expressed to the technical monitors Dr. Walter A. VonRiesemann and Dr. Kenneth J. Saczalski for their support.

References

[1] PILKEY, W., SACZALSKI, K., SCHAEFFER, H., eds., Structural Mechanics Computer Programs, Proceedings of the International Conference of Structural Mechanics Software, University of Maryland, June, 1974, University Press of Virginia, Charlottesville, (1974).

[2] ATLURI, S., WITMER, E. A., LEECH, J. W., MORNIO, L., "PETROS 3: Finite-Difference Method and Program for the Calculation of Large Elastic-Plastic Dynamically-Indeed Deformations of Multilayer Variable-Thickness Shells," Massachusetts Institute of Technology, ASRL TR 152-2, (BRL CR60), (November, 1971).

[3] BALMER, H. A., "Improved Computer Programs--DE-PROSS 1, 2, and 3--to Calculate the Dynamic Elastic-Plastic Two-Dimensional Responses of Impulsively-Loaded Beams, Rings, Plates, and Shells of Revolution," Massachusetts Institute of Technology, ASRL TR 128-3, (August, 1975).

[4] HUFFINGTON, N. J., JR., private correspondence pertaining to REPSIL computer code, (July, 1972.)

[5] HUFFINGTON, N. J., JR., "Large Deflection Elastoplastic Response of Shell Structures," Report No. 1515, Ballistic Research Laboratories, Aberdeen Proving Ground, Md., (1970).

[6] HUFFINGTON, M. R., JR., "Numerical Analysis of Elastoplastic Stress," U. S. Army Ballistic Research Laboratory, Memorandum Report No. 2006, (September, 1969).

[7] BIRNBAUN, M. R., CUPPS, F. J., EMERY, A. F., "SPECTRE--A Finite Difference Computer Program For Calculating the Dynamic Response of A Cylindrical Shell," SCL-DR-70-108, Sandia Laboratories, Livermore, California, (December, 1970).

[8] KRIEG, R. D., DUFFEY, T. A., "UNIVALVE II: A Code to Calculate the Large Deflection Dynamic Response of Beams, Rings, Plates, and Cylinders," Sandia Corporation, Report SC-68-303, (October, 1968).

[9] UNDERWOOD, P., "Transient Response of Inelastic Shells of Revolution," Journal of Computers and Structure, 2, (5-6), pp. 975-989, (December, 1972).

[10] ALMROTH, B. O., BROGAN, F. A., MELLER, E., SELE, F., PETERSON, H. T., "Collapse Analysis for Shells of General Shape; Vol. II--Users Manual for the Stags-A Computer Code," AFFDL TR-71-8, Air Force Flight Dynamic Laboratories, Wright-Patterson Air Force Base, Ohio, (March, 1973).

[11] McNAMARA, J. F., MARCAL, P. V., "Incremental Stiffness Method for Finite Element Analysis of Nonlinear Dynamic Problems," Numerical and Computer Methods in Structural Mechanics, edited by S. J. Fenver, Academic Press, New York, pp. 353-376, (1973).

[12] WU, R. W. H., WITMER, E. A., "Finite-Element Analysis of Large Transient Elastic-Plastic Deformations of Simple Structures, With Application to the Engine Rotor Fragment Containment/Deflection Problem." NASA-CR-120886, National Aeronautics and Space Administration, Washington, D.C., (also ASRL TR 154-4), (January, 1972).

[13] STRICKLIN, J. A., MARTINEZ, J. E., TILLERSON, J. R., HONG, J. H., HAISLER, W. E., "Nonlinear Dynamic Analysis of Shells of Revolution by the Matrix Displacement Method," AIAA Journal 9, (4), pp. 629-636, (April, 1971).

[14] STRICKLIN, J. A., HAISLER, W. E., VON RIESEMANN, W. A., "Large Deflection Elastic-Plastic Dynamic Response of Stiffened Shells of Revolution," Journal of Pressure Vessel Technology, ASME 96, Series J, (2), pp. 87-95, (May, 1974).

[15] HAISLER, W. E., VAUGHAN, D. K., "DYNAPLAS II - A Finite Element Program for the Dynamic, Large Deflection, Elastic-Plastic Analysis of Stiffened Shells of Revolution," TEES-2926-73-2, Aerospace Engineering Dept., Texas A&M University, College Station, Texas, (October, 1973).

[16] VON RIESEMANN, W. A., STRICKLIN, J. A., HAISLER, W. E., "Dynamic Nonlinear Analysis of Shells of Revolution," Paper M 4/6, 3rd International Conference on Structural Mechanics in Reactor Technology, Imperial College, London, (September, 1-5, 1975).

[17] FUNG, Y. C., Foundations of Solid Mechanics, Prentice-Hall, (1965).

[18] ARGYRIS, J. H., Energy Theorems and Structural Analysis, Butterworths, London, (1960).

[19] MALVERN, L E., Introduction to the Mechanics of a Continuous Medium, Prentice-Hall, (1969).

[20] HAISLER, W. E., JR., "Development and Evaluation of Solution Procedures for Nonlinear Structural Analysis," PhD dissertation, Texas A&M University, College Station, Texas, (December, 1970).

[21] HILL, R., The Mathematical Theory of Plasticity, Oxford University Press, Amen House, London, (1950).

[22] DUWEZ, P., "On the Plasticity of Crystals," Physical Review 47, p. 494, (1935).

[23] HUNSAKER, B., VAUGHAN, D. K., STRICKLIN, J. A., HAISLER, W. E., "A Comparison of Current Work-Hardening Models Used in the Analysis of Plastic Deformations," TEES 2926-73-3, Aerospace Engineering Department, Texas A&M University, (October, 73).

[24] DUFFEY, T. A., KEY, S. W., "Experimental-Theoretical Correlations of Impulsively Loaded Clamped Circular Plates," Report SC-RR-68-2]0, Sandia Laboratories, Albuquerque, New Mexico, (April, 1968).

[25] STRICKLIN, J. A., VON RIESEMANN, W.A., TILLERSON, J. R., HAISLER, W. E., "Survey of Static Geometric and Material Nonlinear Analysis by the Finite Element Method," Presented at the Second U.S.-Japan Seminar on Matrix Methods in Structural Mechanics, University of California, Berkeley, California, (August 14-19, 1972).

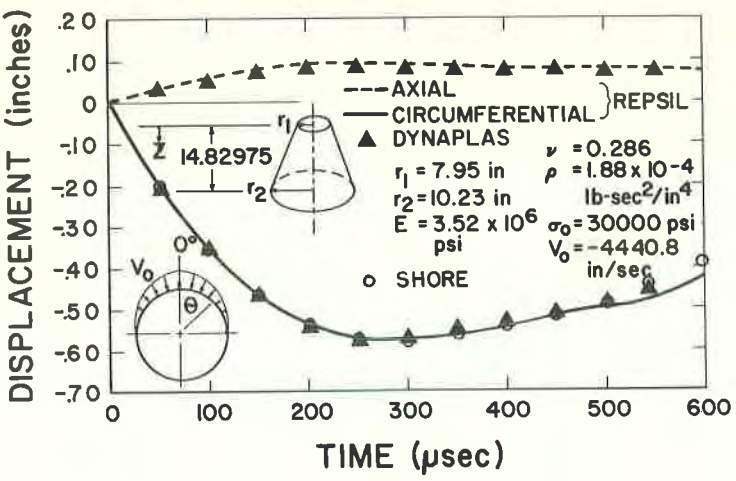

Figure 1 Axial and Radial Displacement For Theta=0^{0} and Z=6.3516 in

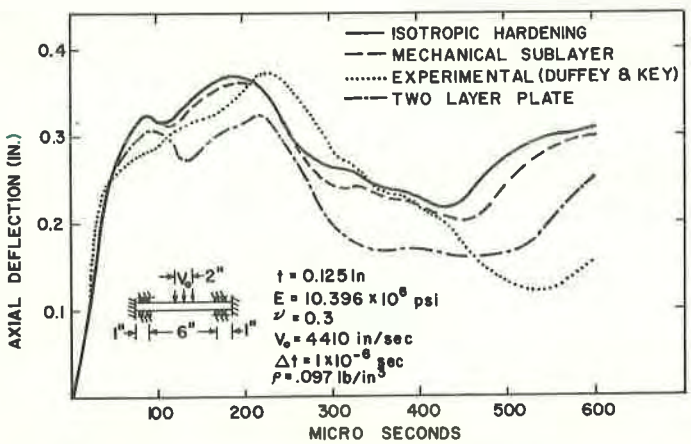

Figure 2 Center Deflection vs. Time For An Impulsively Loaded Circular Plate

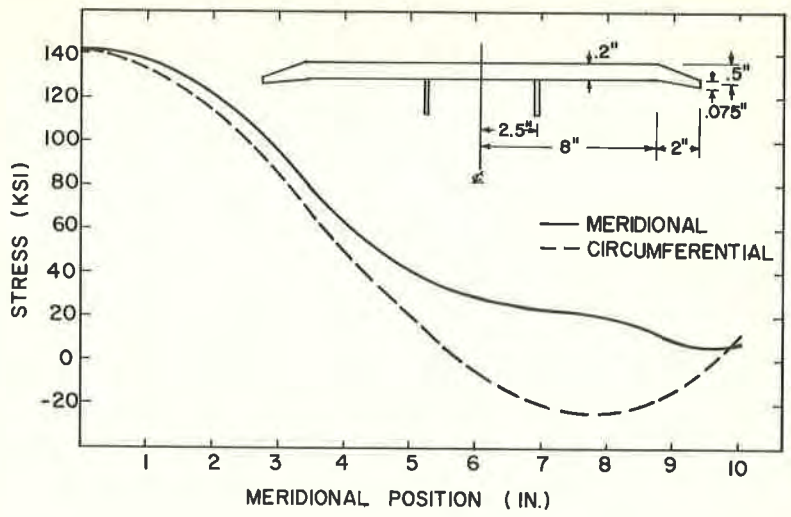

Figure 3 Stress in Thermal Shield At Lower Surface At Time=5.5 Milliseconds

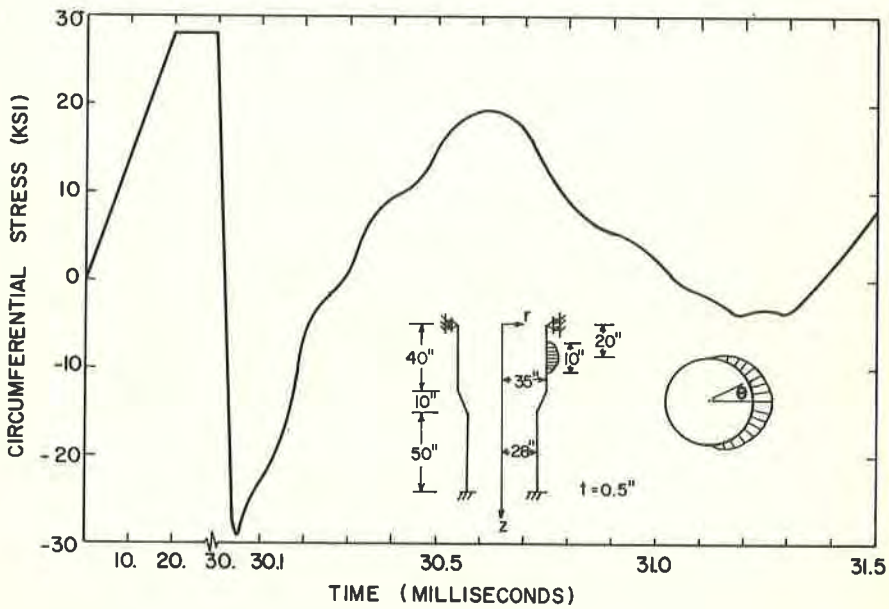

Figure 4 Circumferential Stress Under Thermal Load ($\theta=0^{o}$, Z=20", Outside Surface)

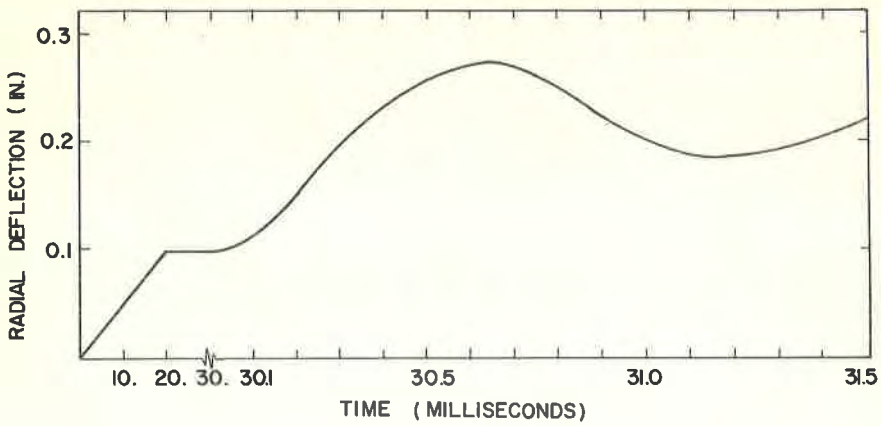

Figure 5 Radial Deflection Under Thermal Load

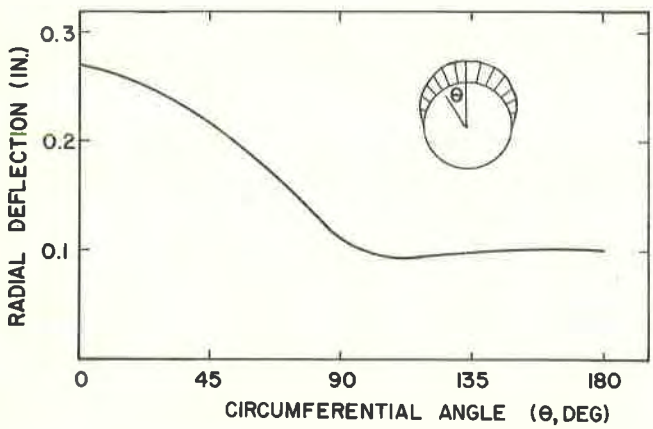

Figure 6 Radial Deflection Under Thermal Load Around Circumference (Z=20", t= 30.66 Millisec)